



Large-signal microwave performance of GaN-based NDR diode oscillators

Egor Alekseev, Dimitris Pavlidis *

*Department of Electrical Engineering and Computer Science, The University of Michigan, 2307 EECS Building,
1301 Beal Avenue, Ann Arbor, MI 48109-2122, USA*

Received 2 December 1999; accepted 5 January 2000

Abstract

The GaN material parameters relevant to the negative differential resistance (NDR) devices are discussed, and their physical models based on the theoretical predictions and experimental device characteristics are introduced. Gunn diode design criteria were applied to design the GaN NDR diodes. A higher electrical strength of the GaN allowed operation with higher doping ($\sim 10^{17} \text{ cm}^{-3}$) and at a higher bias (90 V for a 3 μm thick diode). The transient hydrodynamic simulations were used to carry out the harmonic power analysis of the GaN NDR diode oscillators in order to evaluate their large-signal microwave characteristics. The GaAs Gunn diode oscillators were also simulated for a comparison and verification purposes. The dependence of the oscillation frequency and output power on the GaN NDR diode design and operating conditions are reported. It was found that, due to the higher electron velocities and reduced time constants, GaN NDR diodes offered twice the frequency capability of the GaAs Gunn diodes (87 GHz vs. 40 GHz), while their output power density was $2 \times 10^5 \text{ W/cm}^2$ compared with $\sim 10^3 \text{ W/cm}^2$ for the GaAs devices. The reported improvements in the microwave performance are supported by the high value of the GaN Pf^2Z figure of merit, which is 50–100 times higher than the GaAs, indicating a strong potential of the GaN for the microwave signal generation. © 2000 Elsevier Science Ltd. All rights reserved.

Keywords: GaN and GaAs based; Negative differential resistance (NDR); Gunn diode oscillator; THz capabilities; Transient hydrodynamic (energy-balance) simulations; Harmonic power analysis

1. Introduction

The principle of the negative differential resistance (NDR) has been successfully employed in the semiconductor devices. The GaAs- and the InP-based Gunn diodes, based on the bulk NDR effect, have manifested good characteristics for the microwave and millimeter-wave signal generation [1,2]. The NDR effect in these materials is due to the electron transfer between the high-mobility central and the low-mobility satellite valley. The use of the wide-band-gap semiconductors, such as the GaN, with an increased electrical strength offers the

possibility to increase the output power of the semiconductor devices. Thus, a record output power density for any FET of 7 W/mm at 10 GHz was recently obtained with the GaN-based MODFETs [3]. The studies of the fundamental properties of the GaN indicates that this material also exhibits a bulk NDR effect with a threshold field F_{TH} of the order of 80–150 KV/cm. Various possibilities are suggested for the nature of the NDR in nitrides, including the electron intervalley transfer [4], and the inflection of the central valley [5]. Independent of the nature of the NDR, Gunn domain instability is expected to be possible in a semiconductor provided the appropriate I - V characteristics are present [6].

Although further confirmation is needed regarding the presence of a transferred-electron effect in GaN-based materials, it is important at this stage to evaluate the advantages of using a GaN in the NDR signal generators. The latter include increased the electrical

*Corresponding author. Tel.: +1-734-647-1778; fax: +1-734-763-9324.

E-mail addresses: yegor@umich.edu (E. Alekseev), pavlidis@umich.edu (D. Pavlidis).

strength, a higher threshold field, and the possibility of a faster operation due to the larger electron velocity and a reduced energy-relaxation time in the GaN. This article provides the first systematic analysis of the use of the GaN for the NDR diode realization and discusses the expected frequency and power characteristics of the GaN NDR oscillators as a function of bias, doping, frequency, and termination impedance of the resonant cavity.

2. Modeling of GaN material parameters

The studies of the GaN-based NDR diodes were conducted by employing a commercial semiconductor-device simulator Medici [13]. Since this program does not contain material parameters for GaN, these had to be obtained from the literature and were evaluated, verified, and properly introduced into the simulator. Comparisons of a simulated performance with the experimental characteristics of the GaN-based MESFETs and PIN diodes were made to enable the validation of the selected parameters. Further details on the adopted approach are presented elsewhere [7].

A low-field electron mobility of $\mu_n = 280$ and $60 \text{ cm}^2/\text{Vs}$ were assumed for the wurtzite (Wz) GaN doped at $N = 5 \times 10^{16}$ and $1 \times 10^{19} \text{ cm}^{-3}$, respectively [8]. The values of an electron lifetime $\tau_n = 7 \text{ ns}$ and a hole lifetime $\tau_p = 0.1 \text{ ns}$ used in the simulations were based on the experimental data measured by an electron-beam-induced current method [9]. The coefficients for calculating the impact-ionization rates in the GaN were obtained by fitting the theoretical predictions presented in Ref. [10] and verified by comparing the simulation results with the experimental breakdown voltages reported for the GaN PIN diodes [11].

The models for the field dependence of an electron mobility in the GaN were based on the v - F characteristics calculated by the Monte Carlo simulations [4,12]. The velocity-field characteristics, evaluated in these studies, demonstrated a bulk NDR effect in the high-field region due to the intervalley transfer. However, the threshold field for the intervalley transfer and a consequent appearance of the NDR in a GaN was much larger than in conventional semiconductors such as GaAs. An increase in the threshold field is caused by a larger separation between the satellite and central valleys in the Wz GaN where ΔE is $\approx 2.1 \text{ eV}$ compared to $\Delta E \approx 0.3 \text{ eV}$ for GaAs. The analytical expression (Eq. 1) for v - F characteristics in the GaAs [13] was used in the simulations:

$$v(F) = \mu F \frac{1 + \frac{v_{\text{SAT}}}{\mu F} \left(\frac{F}{F_{\text{TH}}} \right)^4}{1 + \left(\frac{F}{F_{\text{TH}}} \right)^4}. \quad (1)$$

This was fitted to the results of Ref. [12] in order to obtain the v - F dependence on the GaN, which manifests

a higher peak velocity v_{PEAK} (3×10^7 vs. $1.5 \times 10^7 \text{ cm/s}$), increased saturation velocity v_{SAT} (2×10^7 vs. $0.6 \times 10^7 \text{ cm/s}$), and a much larger threshold field F_{TH} (150 vs. 3.5 KV/cm) compared to the GaAs. At the same time, the GaN low-field mobility of $280 \text{ cm}^2/\text{Vs}$ and the peak negative differential mobility $\mu_{\text{NDR}} \equiv \max(-dv/dF)$ of $50 \text{ cm}^2/\text{Vs}$ are lower than the GaAs values of 8000 and $2500 \text{ cm}^2/\text{Vs}$, respectively.

According to recent studies on the GaN bandstructure, the Γ -valley inflection point, at which the group electron velocity is maximal, was found to be located below the lowest satellite valley in both zinc-blende (Zb) [5] and Wz GaN [14]. Although further studies are necessary to confirm this, it is possible that the reduction of the drift electron velocity in the Γ valley caused by carriers becoming energetic enough to approach the inflection point can lead to a bulk NDR. This contrasts with other semiconductors, where intervalley transfer or impact ionization are initiated at a lower field than at the inflection-point NDR [1]. Quantum devices employing superlattice structures to reduce the threshold field of the inflection-based NDR mechanism were first proposed by Esaki [15] and their feasibility has since been confirmed [16].

The reported v - F characteristics of the Zb GaN calculated using Monte-Carlo simulations were based on a band structure containing the Γ -valley inflection point, and the results indicated that the NDR was indeed caused primarily by the dispersion of the electron drift velocity in the Γ valley [5]. The inflection-based NDR manifested a threshold field F_{TH} of 80 KV/cm and peak velocity v_{PEAK} of $3.8 \times 10^7 \text{ cm/s}$ compared with $F_{\text{TH}} = 110 \text{ KV/cm}$ and $v_{\text{PEAK}} = 2.7 \times 10^7 \text{ cm/s}$ calculated in Ref. [4] for an intervalley-transfer-based NDR. However, by far, a more important consequence of the inflection-based NDR is the elimination of the intervalley-transfer relaxation time from the time required for the NDR formation and, thus, there is a possibility of a significantly increased frequency capability for the GaN inflection-based NDR diodes.

Frequency-independent v - F characteristics can be used to describe electron transport in the presence of a time-varying electric field as long as the frequency of the operation f is much lower than the NDR relaxation frequency f_{NDR} defined by expression (2):

$$f < f_{\text{NDR}} = \frac{1}{\tau_{\text{ER}} + \tau_{\text{ET}}}, \quad (2)$$

where τ_{ER} is the energy-relaxation time and τ_{ET} is the intervalley relaxation time. The τ_{ER} can be estimated as the time taken to accelerate the electrons to the threshold energy ΔE [1]:

$$\tau_{\text{ER}} = \frac{\sqrt{2m_{\text{eff}}\Delta E}}{qF_{\text{TH}}} \quad (3)$$

The energy-relaxation time of 0.15 ps calculated for the Wz GaN was 10 times smaller than the GaAs value of 1.5 ps. The intervalley-transfer relaxation time τ_{ET} was evaluated from the results of Monte-Carlo studies of the ballistic transport [17]. By extrapolating the reconstructed $\tau_{ET}(F)$ curves to the point of the threshold field $F = F_{TH}$, the electron intervalley-transfer times τ_{ET} of 7.7 and 1.2 ps were found for GaAs and GaN, respectively.

Based on the results of this straightforward analysis, the NDR relaxation frequency f_{NDR} of the GaAs was found to be ~ 105 GHz in excellent agreement with the experimental and theoretical results [1]. The frequency capability of the GaN-based NDR devices was found superior to that of the GaAs Gunn diodes as indicated by the GaN NDR relaxation frequency f_{NDR} of ~ 700 GHz in the case of the intervalley-transfer-based NDR and ~ 4 THz in the case of the inflection-based NDR (with $\tau_{ET} = 0$ ps).

Since the equation and the frequency-response of the v - F characteristics in the GaN is not yet well determined, both the intervalley-transfer-based NDR of the Wz GaN and the inflection-based NDR of the Zb GaN were considered in order to account for the uncertainty in published v - F characteristics.

The important material parameters for the Wz GaN, Zb GaN, and GaAs are summarized in Table 1. The GaN offers a higher peak and saturation velocities than the GaAs, which leads to a reduced transit time and increased frequency of operation. The threshold and breakdown fields are also larger in the GaN, which allows an operation at a higher bias and leads to an increased output power. Increased frequency response of the high-energy electrons in the GaN is attributed directly to the higher electrical strength of this material compared with the GaAs. The THz capability, predicted for the GaN devices operating on the inflection-based NDR, is possible due to an exceptionally high frequency response of the electrons to the variations in the band-structure as suggested in [16].

3. GaN NDR diode design

When a high electric field $F > F_{TH}$ is applied to a bulk GaN, the electrons experience a negative differential mobility μ_{NDR} . Under these conditions, a non-uniformity

of the electron concentration would grow at a rate of $1/\tau_{DDR}$. τ_{DDR} is known as the differential dielectric relaxation time and is calculated using expression (4):

$$\tau_{DDR} = \frac{\varepsilon}{q\mu_{NDR}N}, \quad (4)$$

where N is the electron concentration, ε is the dielectric constant, and μ_{NDR} is the peak negative differential mobility. It is recognized that domain the growth lasts for at least $3 \times \tau_{DDR}$ [18] and, thus, the operation frequency of the NDR devices can be limited by the active layer doping. The dependence of the frequency capabilities on N for the GaN and GaAs was calculated using the material parameters of Table 1. The negative differential mobility in the GaAs is higher than in GaN, and, therefore, for the low doped devices, growth of the electron domains occurs faster in the GaAs than in GaN. However, as N is increased, the τ_{DDR} is reduced, and the frequency capability improves until it reaches the NDR relaxation frequency f_{NDR} discussed in Section 2. Since $f_{NDR}^{GaAs} < f_{NDR}^{GaN}$ the frequency capability of the GaN-based devices improves for a higher N without being limited by the f_{NDR} as in the case of the GaAs. This leads to GaN NDR operation that exceeds the GaAs limit of 105 GHz for GaN doping levels above $5 \times 10^{16} \text{ cm}^{-3}$.

The $(N \times L)$ criteria for the possibility of the Gunn domain instability are based on the fact that the domain growth rate $1/\tau_{DDR}$ should be higher than the transit frequency $f_T = v_{PEAK}/L_A$:

$$(N_A \times L_A) > (N \times L)_0 \equiv \frac{3 \times \varepsilon \times v_{PEAK}}{q \times \mu_{NDR}}, \quad (5)$$

where N_A is the doping and L_A is the thickness of the active layer and the factor 3 accounts for the domain growth time as explained earlier. The critical values of $(N \times L)$ product for the GaN and the GaAs were calculated using Eq. (5), and the material parameters of Table 1, and the results are summarized in Table 2. The results show that, due to a higher peak velocity and a smaller negative mobility, $(N \times L)_0$ for the GaN is 10–100 times larger than the GaAs.

However, if the N_A exceeds the critical doping concentration N_{CRIT} , the static domains can be formed inside the active layer [18]. The formation of the parasitic static domains results in a decrease of the output power and may lead to an early breakdown. Values of the

Table 1
The semiconductor material parameters of the GaAs and GaN

Material	F_{TH} (KV/cm)	F_B (MV/cm)	v_{SAT} (cm/s)	v_{PEAK} (cm/s)	μ (V/cm ² /s)	μ_{NDR} (V/cm ² /s)	τ_{NDR} (ps)
GaAs	3.5	0.4	0.6×10^7	1.5×10^7	8000	~ 2500	9.4
Wz GaN	150	2	2×10^7	2.9×10^7	280	~ 50	1.4
Zb GaN	80	1.2	1.7×10^7	3.5×10^7	730	~ 220	0.25

Table 2
The $(N \times L)_0$ products and critical doping levels for the GaN and GaAs

Material	GaAs	Zb GaN	Wz GaN
$(N \times L)_0$ (cm ⁻²)	0.1×10^{11}	2.5×10^{12}	8.2×10^{12}
N_{CRIT} (cm ⁻³)	3.4×10^{15}	1.2×10^{18}	4.3×10^{18}

critical doping concentration N_{CRIT} calculated using Eq. (6) for the cases of the GaN and GaAs are also listed in Table 2.

$$N_{\text{CRIT}} = \frac{\epsilon \times F_{\text{TH}}^2}{q} \quad (6)$$

Due to the large difference in the threshold electric fields, N_{CRIT} in the GaN is much higher than in GaAs and, thus, the active region in the GaN diodes can be doped significantly higher ($\sim 10^{17}$ cm⁻³) than in GaAs designs ($\sim 10^{15}$ cm⁻³). The latter is a very important result in terms of the feasibility of the GaN-based NDR diodes, since the availability of the low-doped GaN material ($N_A < 5 \times 10^{16}$ cm⁻³) is still limited. Higher doping of the active layers in the GaN NDR diodes also leads to a reduction of the τ_{DDR} in this material, helping to increase its frequency capability.

A typical GaN NDR diode designed to operate at ~ 100 GHz had an n-type active layer with the thickness L_A of 3 μm and doping N_A of 1×10^{17} cm⁻³. The active layer was sandwiched between the anode and cathode layers and their corresponding ohmic contacts. Both contact layers were 0.1 μm thick and doped at 1×10^{19} cm⁻³. The diameter of the diode D was selected to be 50 μm . A final three-dimensional model of the GaN NDR diode oscillator is shown in Fig. 1 together with the bias supply and a parallel LCR circuit used to represent the resonant cavity.

4. Simulation approach

The custom *hydrodynamic* simulators have previously been used for the study of Gunn diodes [19]. The commercial simulator employed in our work also offers hydrodynamic capabilities, and has been used for a basic

study of a possibility of the Gunn oscillations in the collectors of the GaAs-based HBTs [20]. In this work, in addition to the simulating GaN devices, we extended the capabilities of this simulator to allow a large-signal power characterization of the GaN NDR diode oscillators and, for comparison purposes, the GaAs Gunn diode oscillators.

The equations used in the hydrodynamic simulations of the GaN NDR diodes included Poisson's equation, carrier-continuity equations, and the electron energy-balance equations. By including the NDR relaxation time τ_{NDR} in the energy relaxation time used in the energy-balance equations, NDR in v - F characteristics was constrained to the frequencies lower than the NDR relaxation frequency f_{NDR} .

The static as well as time-dependent coupled solutions of the hydrodynamic equations were obtained by applying Newton's numerical differentiation and integration method to the spatial distributions of the electron concentration, potential, electric field, and electron velocity [13]. A bias application was possible by setting the Fermi level on the boundary between the anode layer and the anode contact equal to the externally applied voltage. During simulations of the GaN NDR diode oscillators, the additional boundary conditions based on the Kirchhoff equations were used to represent a parallel LCR circuit connected between the voltage supply and the anode contact of the GaN NDR diode. The transient large-signal simulations were used to obtain current and voltage waveforms corresponding to the device oscillations. A harmonic power analysis employing Fourier transforms was used to evaluate the output power spectrum and extract the frequency and output power of the GaN NDR diode oscillators.

5. Simulations of GaN NDR diode oscillators

When a bias V_D exceeding the critical value $V_{\text{CR}} = F_{\text{TH}} \times L_A$ is applied to the anode contact, it results in an electric field $F > F_{\text{TH}}$. Under such conditions, the GaN NDR diode may become unstable and give rise to sustained oscillations. The power and frequency of the oscillations depend on the device design, biasing

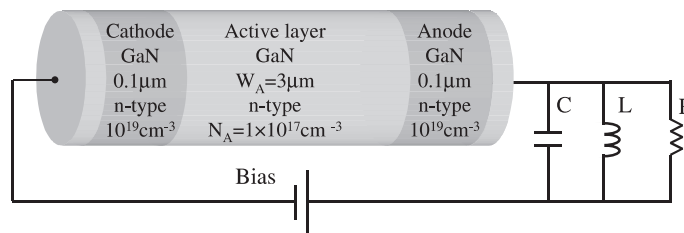


Fig. 1. The schematics of the GaN NDR diode oscillator.

conditions, and termination impedance of the resonant cavity Z_L .

Thus, a nominal Wz GaN NDR diode was biased using $V_D = 2 \times V_{CR}$ and connected to a parallel LCR circuit with $L = 17.5$ pH, $C = 0.1$ pF, and $R = 50 \Omega$. Starting at zero time, V_D was increased from 0 to 90 V with a greater time rise of >1 ns in order to minimize the voltage overshoot. Large-signal transient simulations were used to record the voltage and current waveforms and the results are shown in Fig. 2. The figure shows the emergence of the oscillations in voltage and current when the bias exceeds V_{CR} of 45 V. A gradual build-up of the amplitude of the current oscillations is shown in Fig. 2b (see the inset). The growth of the oscillations takes place over 0.5 ns, and is followed by a region of sustained oscillations. The dynamic load-line corresponding to the sustained oscillations is shown in Fig. 3 together with a stable DC $I-V$ curve simulated for the case when the GaN diode was connected directly to a voltage source. The reduction in the value of the quiescent current observed in this figure is caused by the presence of the sustained oscillations. An experimentally observed NDR in the $I-V$ characteristics of the Gunn-diode oscillators confirms this trend.

The voltage and current waveforms in the region of the sustained oscillations were subjected to the harmonic power analysis and the obtained spectrum of the output power is shown in Fig. 4. The oscillation frequency of

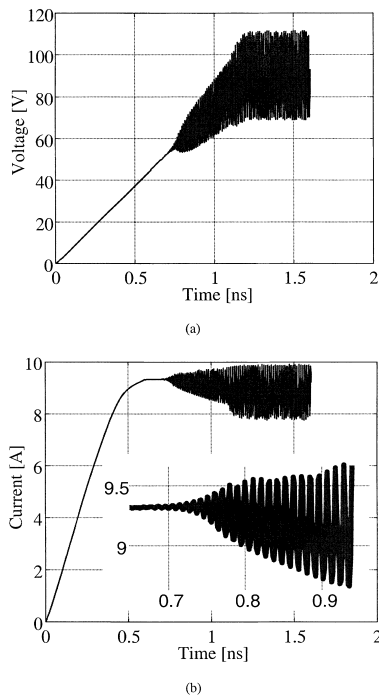


Fig. 2. The voltage and current waveforms of the GaN NDR diode oscillator.

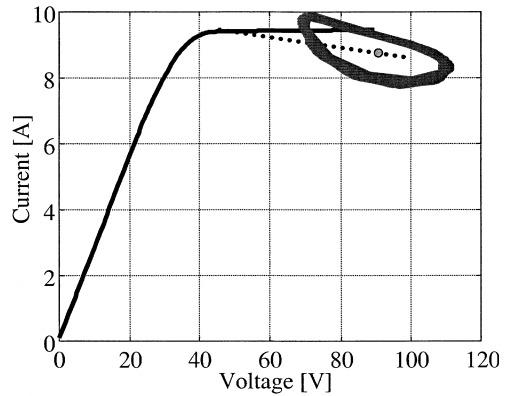


Fig. 3. A dynamic load-line and DC $I-V$ characteristic of the GaN NDR diode oscillator.

the GaN NDR diode oscillator employing 3 μm thick, a 50 μm diameter GaN NDR diode was 87 GHz. Considering the employed LCR circuit parameters and the oscillation frequency, the large-signal capacitance of the GaN NDR diode was found to be ~ 100 fF. The fundamental output power was 37.6 dBm corresponding to the power density of 2×10^5 W/cm², while the conversion efficiency was 0.73%. This modest value of the conversion efficiency compared to the theoretical limit of $\eta = 8/\pi^2 \times (V_{PEAK} - V_{SAT})/(V_{PEAK} + V_{SAT})$ of 15% is attributed to a low value of the quality factor ($R/\omega L = \sim 5.4$) of the LCR circuit used to represent the resonant cavity.

The impact of the biasing voltage on the frequency, output power, and efficiency was investigated using the same Wz GaN NDR diode oscillator (see Fig. 5). The frequency of the oscillations decreased steadily from 98 to 83 GHz as the bias was increased from 55 to 125 V in agreement with the experimental trends observed for the

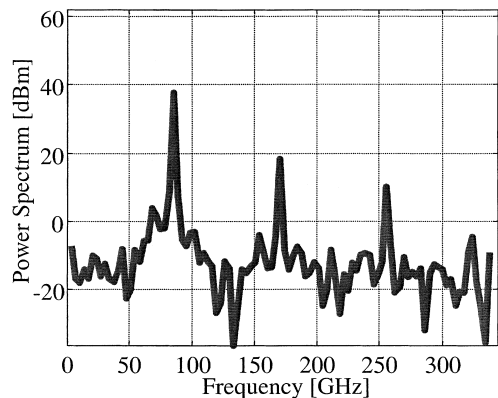


Fig. 4. An output power spectrum of the GaN NDR diode oscillator.

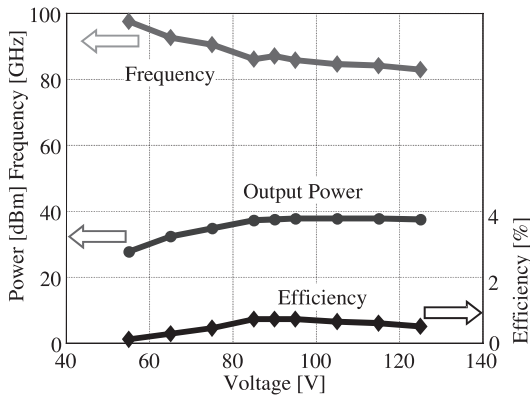


Fig. 5. A variation of the output power, frequency, and efficiency of the GaN NDR diode oscillator with bias.

GaAs Gunn diodes [21]. The output power increased steeply once the applied bias exceeded V_{CR} , and saturated for $V_D > 2 \times V_{CR}$. A slow decrease for $V_D > 3 \times V_{CR}$ is attributed to an ensuing mismatch between the large-signal impedance of the GaN NDR diode and the terminating impedance Z_L . The conversion efficiency was maximal for $V_D = 2 \times V_{CR}$ and this bias was employed for performing comparative studies of the various GaN NDR diode oscillators.

The power and frequency capabilities of the GaN NDR diodes were compared with that of the GaAs Gunn diodes by simulating the performance of the corresponding oscillators while modifying the thickness L_A and the doping N_A of the active layer in these devices. The nominal GaAs Gunn diode had the same dimensions as the nominal GaN NDR diode: $L_A = 3 \mu\text{m}$ and $D = 50 \mu\text{m}$, but the doping was reduced to $3 \times 10^{15} \text{ cm}^{-3}$ in order to satisfy the design condition $N_A < N_{CRIT}$ (Table 2). This design of GaAs Gunn diode was analogous to published descriptions of Ka-band Gunn diodes in Ref. [22]. The bias V_D for both the GaN- and GaAs-based devices was selected to be twice the critical bias V_{CR} and, for the nominal designs, was 90 V and 2.1 V, respectively. Designs of the LCR circuits for the GaN ($L = 17.5 \text{ pF}$, $C = 0.1 \text{ pF}$, $R = 50 \Omega$) and the GaAs ($L = 25 \text{ pF}$, $C = 0.45 \text{ pF}$, $R = 50 \Omega$) were optimized to provide the maximum output power when used with the devices of the nominal designs.

The results of the study conducted by varying the thickness of the active layer are shown in Fig. 6. All devices demonstrated expected trends of increasing the oscillation frequency and decreasing the output power when the thickness of the active layers was reduced. Reduction of the output power for the GaN NDR diodes with thicker than $3 \mu\text{m}$ active layers was due to an increasing mismatch with the resonant cavity. An even more significant degradation was observed for the GaAs Gunn diodes and special care was taken in that case to

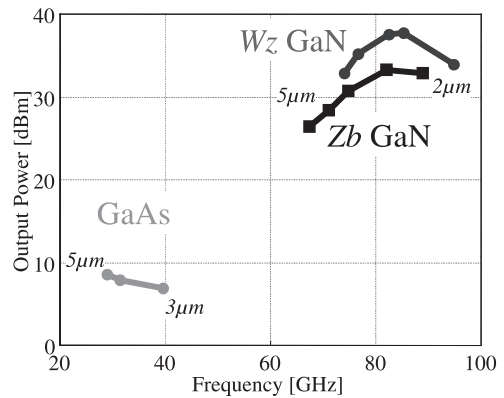


Fig. 6. The power-frequency diagram for the GaN NDR diode and GaAs Gunn diode oscillator for the devices with an active layer width between 2 and $5 \mu\text{m}$.

re-optimize the Z_L for devices with thicker active layers. The frequency–power tradeoff of the GaAs Gunn diodes was restored by proper choice of a Z_L and only the re-optimized results are shown in Fig. 6.

The simulations were conducted for the NDR diodes made of both Wz and Zb phases of the GaN in order to account for the uncertainty in published v – F characteristics. The simulations showed that the overall characteristics of the GaN-based NDR diodes outperform those of the GaAs Gunn diodes in terms of output power and frequency of oscillations independent of the specific v – F characteristics used to model material properties of the GaN. Thus, given the same thickness of the active layer, the operation frequency of the GaN NDR diodes (65–95 GHz) was approximately twice as that of the GaAs Gunn diodes (27–40 GHz), while given the same device area, the maximum output power of the GaN NDR diodes was $\sim 35 \text{ dBm}$ compared with $\sim 10 \text{ dBm}$ for the GaAs Gunn diodes.

The power–frequency capability of the GaN NDR diodes was also studied as a function of the doping of the active layer. When the N_A was increased from 5×10^{16} to $5 \times 10^{17} \text{ cm}^{-3}$, the oscillation frequency was increased from 85 to 120 GHz due to a reduced differential dielectric relaxation time in the higher-doped devices.

On the whole, when compared to the GaAs Gunn diodes, the GaN NDR diodes showed a significant improvement in terms of output power density and frequency. These results were supported by similar conclusions drawn with the help of the microwave signal generator figure-of-merit $Pf^2Z = F_B^2 v_{PEAK}^2 / 4$, which measures the maximum output power (P) delivered from an oscillator to a matched impedance (Z) at a frequency (f) [1]. Based on the considered material properties, Pf^2Z for GaN is 50–100 times that of the GaAs, indicating a strong potential of the GaN for a microwave signal generation.

6. Conclusions

The GaN-based NDR diodes were introduced and the physical models for the relevant material parameters of the Wz and Zb phases of the GaN were developed. It was found that due to a higher electrical strength and reduced time constants, the GaN NDR diodes offered a higher increased frequency and power capability compared with the GaAs Gunn diodes. The microwave characteristics of the GaN NDR diode and GaAs Gunn diode oscillators were evaluated by performing a large-signal harmonic power analysis of the current and voltage waveforms corresponding to the sustained oscillations. The analysis showed that the GaN-based NDR diodes outperform the GaAs Gunn diodes independent of the specific v - F characteristics used to model material properties of the GaN. Thus, given the same thickness of the active layer, the frequency capabilities of the GaN NDR diodes (65–95 GHz) was approximately twice that of the GaAs Gunn diodes (27–40 GHz), while their output power density ($\sim 10^5$ W/cm²) was at least 100 times higher than that of the GaAs devices. The strong potential of the GaN for a microwave signal generation is supported by the Pf^2Z figure of merit for the GaN, which is 50–100 times higher than the GaAs. The improvements offered by the wide-gap semiconductor are due to a significantly higher electrical strength which allows an operation with higher doping levels and at a higher bias, than in a conventional narrow-gap III–V semiconductors.

Acknowledgements

This work was supported by ONR under contract Nos. N00014-92-J-1552 and N00014-99-1-0513.

References

- [1] Eisele H, Haddad GI. Active microwave diodes. In: Sze SM, editor. Modern semiconductor device physics. New York: Wiley, 1998.
- [2] Bulman PJ, Hobson GS, Taylor BC. Transferred electron devices. London and New York: Academic Press, 1972.
- [3] Sheppard ST, Doverspike K, Pribble WL, Allen ST, Palmour JW, Kehias LT, Jenkins TJ. High power microwave GaN/AlGaIn HEMTs on semi-insulating silicon carbide substrates. IEEE Electron Dev Lett 1999;20(4):161–3.
- [4] Kolnik J, Oguzman IH, Brennan KF, Rongping W, Ruden PP, Yang W. Electronic transport studies of bulk zinc-blende and wurtzite phases of GaN based on an ensemble Monte Carlo calculation including a full zone band structure. J Appl Phys 1995;78(2):1033–8.
- [5] Krishnamurthy S, van Schilfgaarde M, Sher A, Chen AB. Bandstructure effect on high-field transport in GaN and GaAlN. Appl Phys Lett 1997;71(14):1999–2001.
- [6] Ridley BK. Specific negative resistance in solids. Proc Phys Soc 1963;82(12):954.
- [7] Alekseev E, Pavlidis D. DC and high-frequency performance of AlGaIn/GaN heterojunction bipolar transistors. Solid St Electron 2000;44(2):245–52.
- [8] Mohammad SN, Morçoç H. Progress and prospects of group-III nitride semiconductors. Prog Quant Electr 1996;20(5/6):361–525.
- [9] Bandic ZZ, Bridger PM, Piquette EC, Beach RA, Phanse VM, Vaudo RP, Redwing J, McGill TC, DenBaars S, Palmour J, Shur M, Spencer M. Nitride based high power devices: transport properties, linear defects and goals. Wide-Bandgap Semiconductors for High Power, High Frequency and High Temperature. Symp Mater Res Soc, Warrendale, PA, USA 1998;512:27–32.
- [10] Kolnik J, Oguzman IH, Brennan KF, Rongping W, Ruden PP. Monte Carlo calculation of electron initiated impact ionization in bulk zinc-blende and wurtzite GaN. J Appl Phys 1997;81(2):726–33.
- [11] Dmitriev VA, Kuznetsov NI, Irvine KG, Carter Jr. CH, Ponce FA, Dupuis RD, Nakamura S, Edmond JA. Electric breakdown in nitride pn junctions. Gallium Nitride and Related Materials. First Int Symp Mater Res Soc, Pittsburgh, PA, USA 1996;395:909–12.
- [12] Bhapkar UD, Shur MS. Monte Carlo calculation of velocity-field characteristics of wurtzite GaN. J Appl Phys 1997;82(4):1649–55.
- [13] MEDICI, two-dimensional device simulation program, version 2.3, user's manual, February 1997, Technology Modeling Associates, CA.
- [14] Chen AB, (see also Ref. [5]): private communications.
- [15] Esaki L, Tsu R. Superlattice and negative differential conductivity in semiconductors. IBM Journal R & D 1970;14(1):61–5.
- [16] Schomburg E, Grenzer J, Hofbeck K, Blomeier T, Winnerl S, Brandl S, Ignatov AA, Renk KF, Pavelev DG, Koschurinov Yu, Ustinov V, Zhukov A, Kovsch A, Ivanov S, Kopev PS. Millimeter wave generation with a quasi planar superlattice electronic device. Solid St Electron 1998;42(7–8):1495–8.
- [17] Foutz BE, Eastman LF, Bhapkar UV, Shur MS. Comparison of high field electron transport in GaN and GaAs. Appl Phys Lett 1997;70(21):2849–51.
- [18] Shur M. GaAs devices and circuits. New York and London: Plenum Press, 1987.
- [19] Zyburra MF, Jones SH, Tait GB, Jones JR. 100–300 GHz Gunn oscillator simulation through harmonic balance circuit analysis linked to a hydrodynamic device simulator. IEEE Microwave Guided Wave Lett 1994;4(8):282–4.
- [20] Posse VA, Jalili B. Gunn effect in heterojunction bipolar transistors. Electron Lett 1994;30(14):1183–4.
- [21] Haydl WH. Fundamental and harmonic operation of millimeter wave gunn diodes. IEEE Trans Microwave Theory Tech 1983;31(11):879–89.
- [22] Ruttan TG. High-frequency gunn oscillators. IEEE Trans Microwave Theory Tech 1974;MTT-22(2):142–4.